1.0 Cover page

Assessing the Hazard of Large Aftershocks in Alaska

Award Number: G15AP00049

PI: Dr. Debi Kilb

Scripps Institution of Oceanography/IGPP MC 0225
University of California, San Diego
La Jolla, California 92093-0225 USA

Tele: (858) 822-4607 FAX: (858) 534-6354
E-mail: dkilb@ucsd.edu

Project duration: April 2015 through March 2016

Research supported by the U.S. Geological Survey (USGS), Department of the Interior, under USGS award number G15AP00049*. The views and conclusions contained in this document are those of the authors and should not be interpreted as necessarily representing the official policies, either expressed or implied, of the U.S. Government.*

2.0 Abstract

The seismological community does not yet have an operational plan in place to issue aftershock probability forecasts following a large damaging earthquake in subduction zone regions such as Alaska. Because the bulk of statistical aftershock analyses have been conducted using earthquakes on California crustal strike-slip faults, exporting probability forecast algorithms from California to subduction zones environments might not be appropriate. Here, we generate mainshock/aftershock statistics with the aim to assist future earthquake forecasting efforts in subduction zones. To begin, we identifed all M≥6.5 earthquakes in Alaska within the last ~20 years (1995-2015) in the ANSS Comprehensive Catalog (ComCat) catalog, which net a set of 50 quakes. Of these, we reduced the dataset to 43 sequences that have clearly defined aftershock sequences (i.e., events that are not pre-shocks or aftershocks of other sequences). For each of these 43 sequences we determine the magnitude differential (Δmag) between the mainshock and largest aftershock (a ~1.2 value is expected based on Bath's law) and use a maximum likelihood method to estimate the b-value (a magnitude frequency distribution measurement). Of the 43 sequences, 27 have robust Δmag values that are not subject to change when the aftershock space and time windows are varied within 30 days and 2°. Robust B-values (standard deviations ≤ 0.2) are only found for 7 sequences. These 7 B-values show no obvious correlation with depth or Δmag, although the dataset is too sparse to yield any strong conclusion. We find the magnitude differentials span a wide range (0.1 to 2.7 units) and the median value is 1.1, which is consistent with the expected 1.2 global average value suggested by Bath's law. For the shallow mainshocks (depths ≤ 50 km) there is no obvious dependence between Δmag and mainshock depth, but we find the two deepest events (135 km on 28 July 2001; 109 km on 23 June 2014) have some of the largest differentials. This spatial partitioning suggests it is worthwhile to tune aftershock probability forecasts for subduction zones.

3.0 Main body of the report.

INTRODUCTION

One of the first things the public wants to know after a large earthquake is if aftershocks are expected, how large the aftershocks might be and when they will occur. To address these concerns one key hazard forecasting tools is an aftershock probability report that includes the probability of a strong and possibly damaging aftershock and the probability that an earthquake equal to or larger than the mainshock will occur. For large California earthquakes, the initial auto-generated statement that is posted on the USGS web page is: "there is a 5%-10% chance of a larger earthquake occurring". These reports are issued immediately following California mainshocks and updated as new data and information is obtained [Gerstenberger et al., 2005; Glasscoe et al., 2014]. These statistics are derived from Omori and Gutenberg-Richter relationships and assume earthquake rates are Poissonian [Reasenberg and Jones 1989; Felzer et al., 2003]. Although tools to issue these aftershock probability reports are in place for California, they have yet to be implemented in other seismically active regions such as Alaska and Cascadia.

It is important to put in place tools and information to assist in generating aftershock probability reports, especially because Alaska has the potential to have M>9 earthquakes, some of the largest in the world (Figure 1), and the expected aftershocks could be large as well (magnitude ~8). These large aftershocks themselves are hazardous and can pose a tsunami risk. Because the repeat time between large earthquakes in Alaska is relatively small compared to elsewhere in the US, Alaska data is more appropriate for this type of study, especially in comparison with regions such as Cascadia, which is not as seismically active.

The overall question we address here is how can we use information from past large mainshock/afterschock sequences in Alaska (last ~20 years) to help inform and improve how we issue Alaska aftershock probability reports. To accomplish this we catalog difference in magnitude between mainshock events and their largest aftershocks. Based on Bath's law, the expected mean global average of this magnitude differential is ~1.2 magnitude units [Bath, 1965]. We also determine B-values for each mainshock-aftershock sequence. We explore these results to determine if there are any temporal or spatial correlations between the parameters, and to determine if the magnitude differentials and b-value estimates (i.e., a measurement of the magnitude-frequency relationship) correlate.

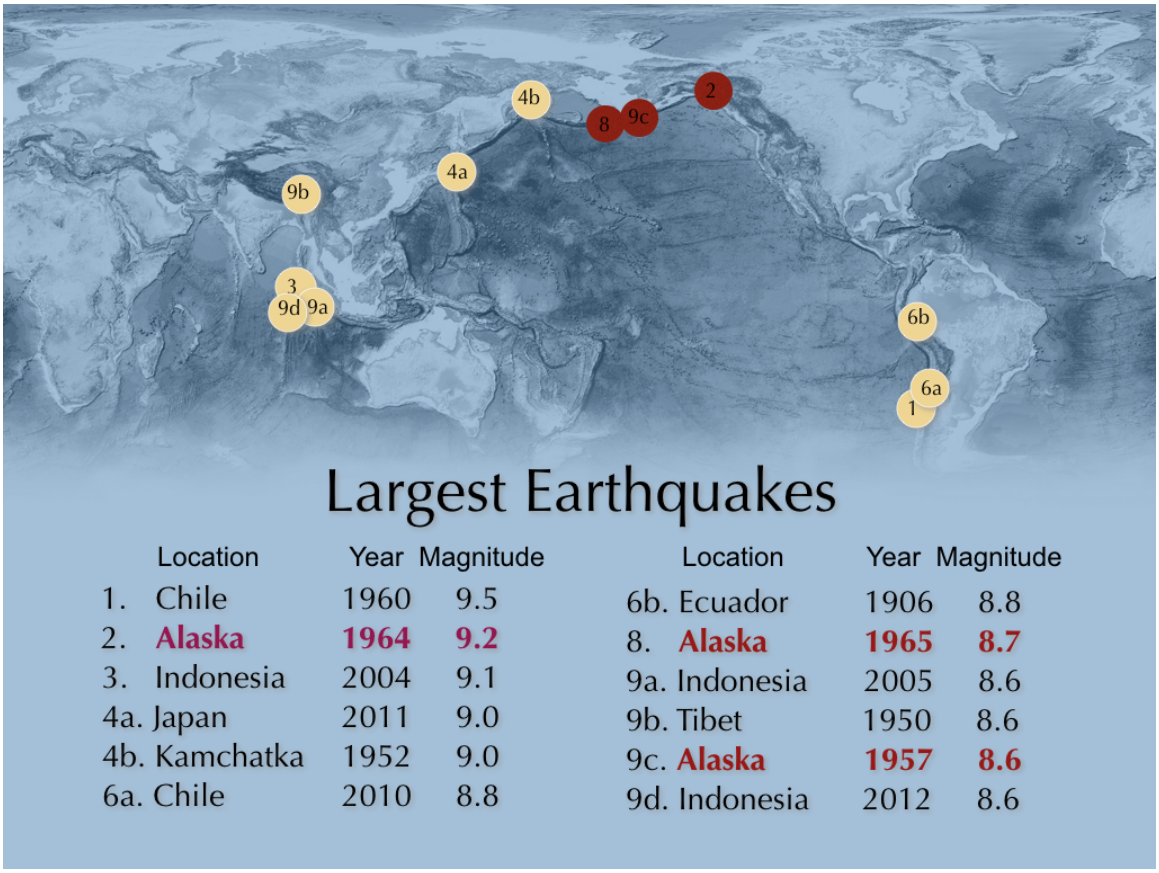

Largest Earthquakes

	Location	Year	Magnitude		Location	Year	Magnitude
1.	Chile	1960	9.5	6b.	Ecuador	1906	8.8
2.	**Alaska**	**1964**	**9.2**	8.	**Alaska**	**1965**	**8.7**
3.	Indonesia	2004	9.1	9a.	Indonesia	2005	8.6
4a.	Japan	2011	9.0	9b.	Tibet	1950	8.6
4b.	Kamchatka	1952	9.0	9c.	**Alaska**	**1957**	**8.6**
6a.	Chile	2010	8.8	9d.	Indonesia	2012	8.6

Figure 1. Largest recorded earthquakes. We list the top 10 events, however, if two events have the same magnitude they are listed with the same number and an identification letter (as in 4a and 4b) and the next number (in this example 5) is not listed because of the previous tie. Note that the only USA quakes that make the list are in Alaska, and that Alaska makes the list three times (red text and map markers). Alaska and Indonesia are the only locations to make the list three times. The three largest events in Alaska occurred near Anchorage (1994), Rat islands (1965) and Andreanof Islands (1957) (data from: http://earthquake.usgs.gov/earthquakes/states/10_largest_us.php).

Alaska data are optimal for exploring these topics because there are far more data from the Alaska region than the entire lower-48 combined. These data have not been mined to their potential as only a few studies provide a comprehensive analysis of Alaskan mainshocks/aftershocks sequences [e.g., Skyes, 1971]. Another benefit is that Alaska includes deep subduction zones as well as shallow strike-slip zones, which will allow us to test the theory that faulting regime plays a role in the magnitude differentials and b-value characteristics. The vast data set will also provide an opportunity to improve our understanding of the physics of subduction zones and make comparisons between Alaska data results and results from other subduction and strike-slip regions [Shearer, 2012; Shcherbakov, et al. 2013; Gomberg and Sherrod, 2014] and potentially inform aftershock forecasts in Cascadia, which has a far smaller earthquake catalog that makes aftershock statistical measurements challenging.

Tectonics of Alaska

Alaska and the Aleutian arc host a >2500 km long subduction zone, numerous active intraplate and plate boundary crustal faults, and 99% of the seismic energy released in the United States over the past 50 years. The sheer size of the Alaskan subduction zone and extensive crustal faulting zones, including the Castle Mountain and Denali Faults, offer fault segments in every phase of the earthquake cycle.

In southeastern Alaska the tectonic motion is dominantly transform in nature, including the Fairweather-Queen Charlotte transform plate interface. Moving into southcentral Alaska, the plate interface transitions to trench normal collision and subduction. This region is tectonically complicated and includes a combination of folding and thrusting and shallow subduction of both the Pacific Plate as well as a microplate (the Kule plate or Yakutat Terrane). Proceeding westward along the Aleutian magathrust the interface between the Pacific and North American plates transitions from subduction under continental crust to subduction under oceanic crust and has an increasing shear component and increasing plunge. The convergence rates increase along the plate boundary as one moves from the east to west and the age of the subducting plate increases as well from ~35 - 63 Ma [DeMets et al., 1994; Ruppert et al., 2007; Freymueller et al., 2008]. Several authors have confirmed the spatial variability in the amount the plate interface is locked or freely slipping across the arc [Freymueller et al., 2008; Freymueller, 2012; Elliott et al., 2013]. Variation in the occurrence of tectonic tremor across the arc hints at variable frictional properties at the base of the locked zone as well [e.g., Peterson et al., 2009; Gomberg and Prejean, 2013].

Alaska Seismic Data from the ANSS ComCat Catalog

Within our study region (-188<longitude<-120.5; 45.5<latitude<75.0) the ANSS Comprehensive Catalog (ComCat) includes 14,725 events magnitude 4 and above in the years 1900-2015. The completeness level of these data vary with time. Levels for the time periods 1975-1995 and 1995-2015 are approximately 4.8 and 4.2, respectively. The completeness level prior to 1975 was much higher, at ~5.5. Given this variability, we focus our work only on data recorded between 1995-2015, which reduces our data to 8441 events M≥4 (Table 1; Figure 2). Of these 8441 events, 50 events are magnitude 6.5 or over (see Table A in Appendix A).

Table 1: Magnitude distribution of 8441 events in the ComCat ANSS catalog (1995-2015, M≥4 events). These 20 years of data are from the region -190≤longitude≤-120; 45≤lattitude≤75. Of these earthquakes, 50 events are magnitude 6.5 or above.

Magnitude Range	Number of events in the ANSS catalog in our study region
4≤M<5	7272
5≤M<6	1044
6≤M<7	113
7≤M<8	12

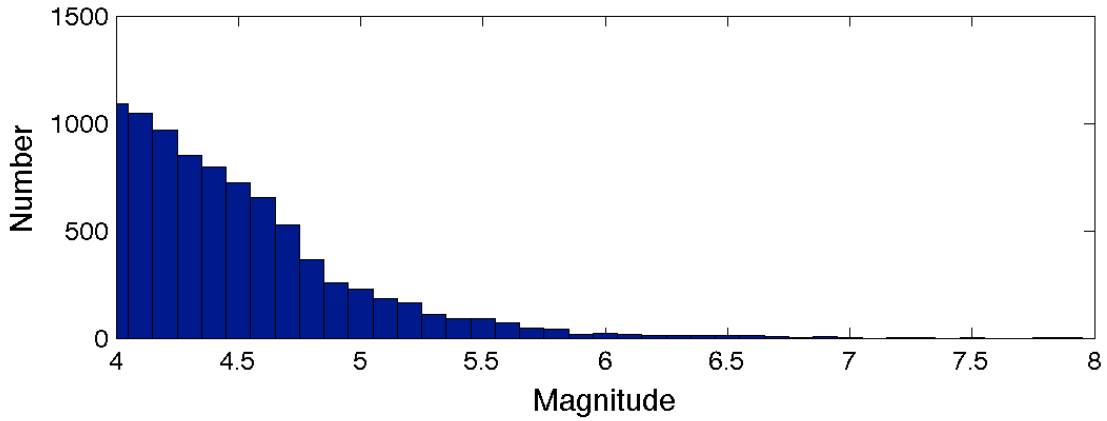

Figure 2. Histogram of earthquake magnitudes for data presented in Table 1, which includes 8441 events from our study region (1995-2015).

Method: magnitude differential and b-value

This work is based on two main parameters. The first is the magnitude differential between a mainshock and it's largest aftershock:

$$\Delta mag = Mmain - Mas \quad (1)$$

where Mmain is the magnitude of the mainshock and Mas is the magnitude of the largest aftershock in the sequence. Bath's law states that within a mainshock-aftershock sequence the Δmag will be on average 1.2 magnitude units [Bath, 1965; Console et al., 2003; Helmstetter and Sornette, 2003]. This 1.2 differential is a mean global average, and variations from this average value will be found in individual sequences and will also depend somewhat on the mean aftershock activity rate. Bath's law has no specific restrictions on the time/space windows used in the computations and so this also introduces some uncertainties in how the values are computed [Shearer, 2012; Hanizl, 2013]. Bath's law is of importance to emergency responders because it can be used as a rule-of-thumb to estimate what the expected magnitude will be of the largest aftershock in sequence.

The second parameter we use is b-value (Figure 3). The b-value is a measure of to what extent there are more small earthquakes than big earthquakes, a magnitude-frequency relationship consistent with a power law:

$$\log10(N) = a - b * Ms \quad (2)$$

where N is the number of earthquakes of magnitude Ms$\pm\Delta$M and b, also called the B-value, is typically 0.8-1.2 [Gutenberg and Richter, 1944]. A B-value of 1 indicates a factor of 10 increase in the number of events for every unit of magnitude decrease (e.g., for every M=6 earthquake there are 10 M=5 earthquakes and 100 M=4 earthquakes etc.). It has been suggested that B-values vary with tectonic setting and different

portions of the fault [Wiemer and Wyss, 2002; Schorlemmer et al., 2005; Ghosh et al., 2008] and that B-values might signal the state of stress of a fault and can potentially be used as a stress-meter that can lead to improved earthquake forecasting [Tormann et al., 2014]. If true, this would allow comparisons of the stress state of different faults and potentially also track the changes in the state of stress as a function of time [Tormann et al., 2014]. In this work we compute B-values using the maximum likelihood method [Aki, 1965; Bender, 1983]. This method is preferred over other methods, such as least squares, because it correctly assumes the error at each point is Poissonian [Felzer, 2006].

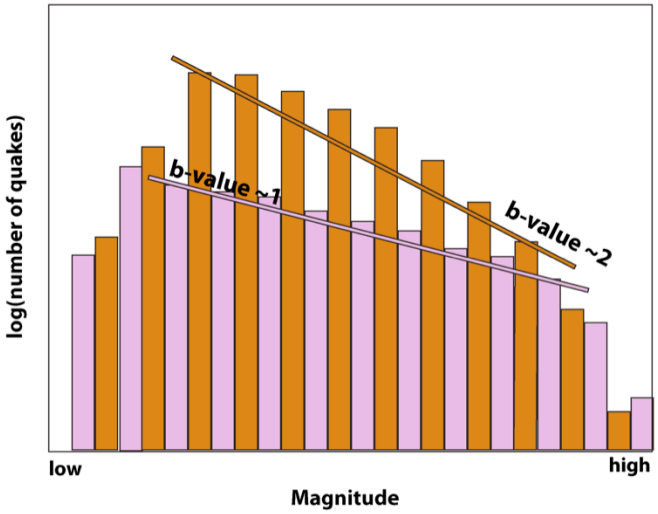

Figure 3. Cartoon of b-values, which are typically 0.8-1.2 [Gutenberg and Richter, 1944]. A lower b-value (pink) indicates a relatively higher population of larger events than smaller events, whereas a high b-value (orange) indicates relatively more small events than big events. Figure modified from Wessels et al. [2011].

RESULTS

Within the last 20 years (1995 – 2015) there were 50 earthquakes magnitude 6.5 or greater (see Table A in Appendix A below). Of these 50 mainshocks, we identified 7-paris of events that are within 2 weeks and a mapped distance of 0.5° of each other. For these pairs we determine which events are pre-shocks (first of the pair has the smallest magnitude, 4 events) and which are aftershocks (second of the pair has the smallest magnitude, 1 event), which we flag for removal from our mainshock catalog. We also remove the two magnitude 6.7 earthquakes that both occurred on 22 March 1996 that were within 0.2° of each other. This leaves us with 43 mainshocks in our data set for consideration (see Table A in Appendix A).

The non-uniform station coverage and deep subduction zone in Alaska and the fact that ~22% of the earthquakes in our data set are assigned depths of 33km makes it difficult to devise a one-size-fits-all clustering algorithm to identify aftershocks of each mainshock. Because of this we take an alternative approach in identifying aftershocks by focusing on determining which sequences have easy to define aftershocks, where the largest aftershock in the sequence is not subject to change when we apply different

space/time windows. We prefer this approach to complicated clustering schemes because it adds an additional assurance that our Δmag values are robust.

Identification of mainshocks with robust Δmag: To identify mainshock/aftershock sequences that have robust Δmag values we use two different tests. In the first test we fix the spatial extent of the aftershock sequence to a circular map-view distance of ±2° from the mainshock, imposing no depth constraints. We then allow the time window to vary up to 30 days and examine the variation in Δmag. If we find the Δmag variation exceeds 0.2 units, we flag the event for removal (Figure 4). Our second test is similar, where instead we hold the time window fixed at 30 days and explore how Δmag changes as we increase the spatial extent out to a maximum of ±2° from the mainshock.

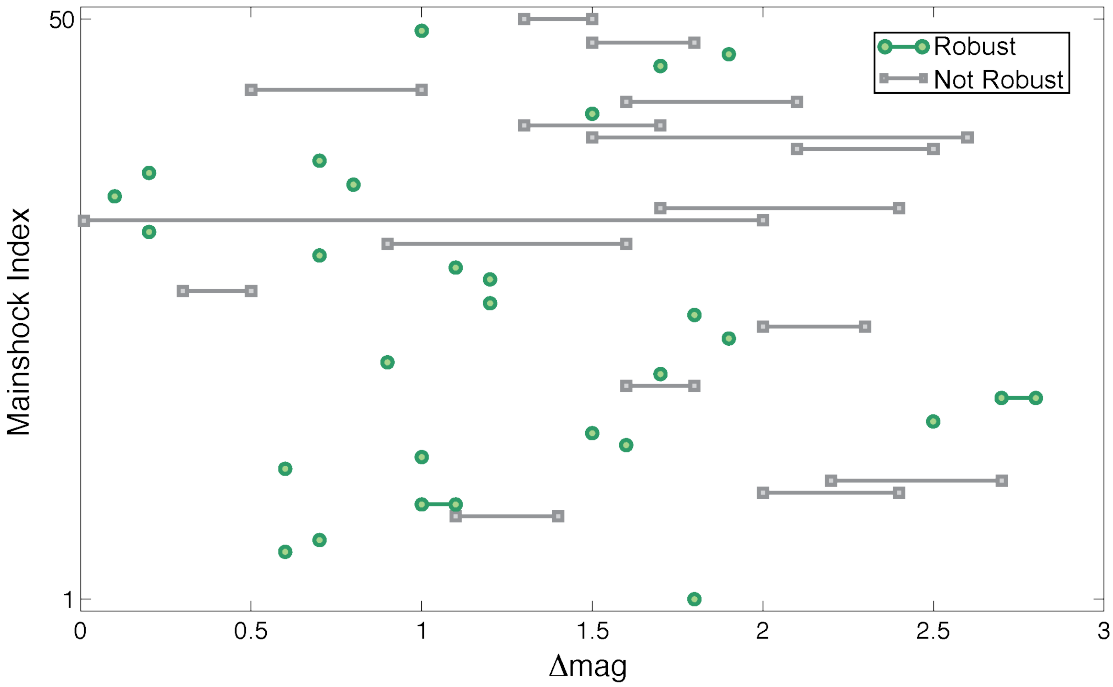

Figure 4: Varying the time window up to 30 days (spatial extent from the mainshock is fixed at ±2°). Mainshock index on the y-axis (as in Table A in Appendix A) and range of Δmag on the x-axis. If the Δmag variation exceeds 0.2 units, we flag the event for removal (in grey) because the Δmag result is too dependent on the selected time window. A similar test (not shown) was done holding the time-window fixed and varying the spatial footprint of the sequences.

Of the 43 sequences considered, 27 have robust Δmag values based on our space and time test. For these mainshocks (6.5 ≤M≤ 9.2) the Δmag span is large, ranging from 0.1 to 2.7 units. The median value, however, is 1.1, which is consistent with the expected 1.2 global average value suggested by Bath's law [Lombardi, 2002]. For shallow events (depths < 50 km) we find no obvious dependence between Δmag and mainshock depth. But, for our 2 deepest events (depths>100km) there is a tendency for the sequences to have relatively higher Δmag values (Figure 5, right side). A map of

these Δmag values weakly suggests a tendency for lower differentials for events in the Aleutians, higher differentials in south-central Alaska and average differentials in southeast Alaska (Figure 5, left side).

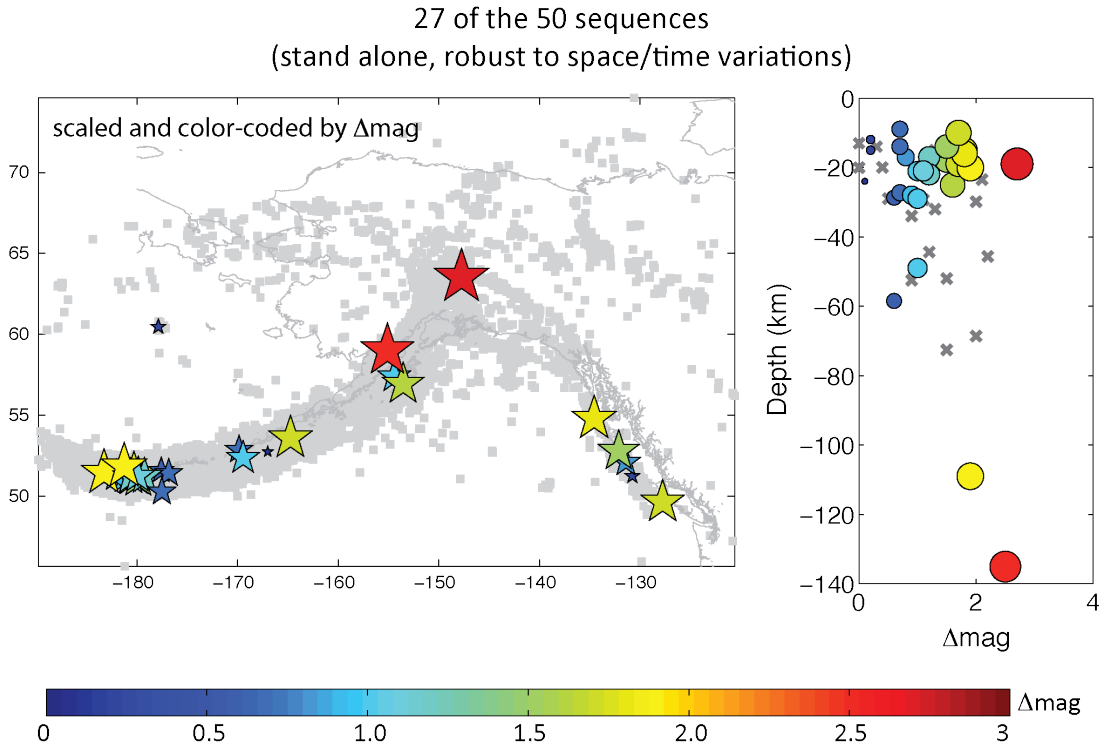

Figure 5: Results, color-coded and sized by Δmag where warmer (cooler) colors indicate higher (lower) Δmag values. These select 27 mainshocks weakly suggest a tendency for lower differentials for events in the Aleutians, higher differentials in south-central Alaska and average differentials in southeast Alaska. These events show no obvious dependence on mainshock depth for shallow events (≤50 km), and relatively higher Δmag for deeper events (depths that exceed 100 km).

B-value Computations: Next, using the maximum likelihood method described above, we compute B-values. We first reduce our favored 27 sequences to only those that have at least 50 aftershocks, resulting in 13 sequences. Computing B-values for these 13 sequences we find the standard deviations can be quite large. Therefore, for our final dataset we only select sequences that have well constrained B-values (standard deviations ≤ 0.2). This process results in only 7 sequences (those highlighted in orange in Table A in Appendix A).

Correlation between magnitude differentials and b-values: Our dataset is too sparse, only 7 sequences, to determine if B-values fluctuate with time/space and track the correlations between B-values and other parameter values (Figure 6).

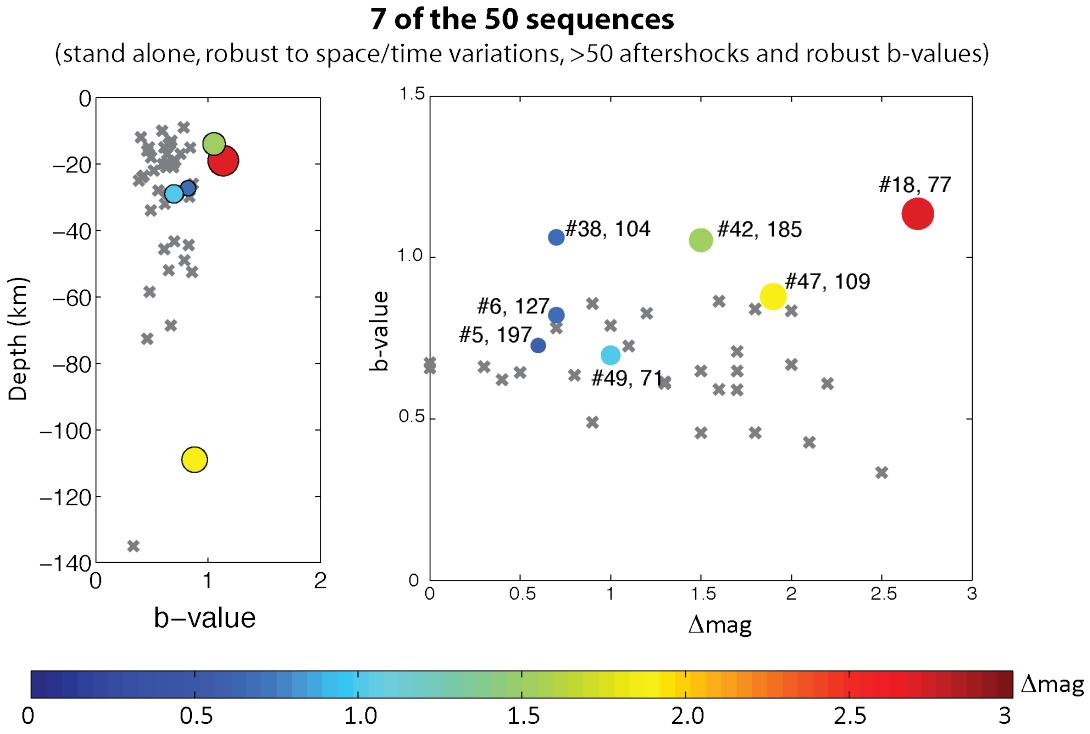

Figure 6: Results from the 7 sequences with robust b-values, where the first number is the index number (see Table A in Appendix A) and the second number is the number of aftershocks in the sequence. Although 7-sequences is too sparse to make any strong conclusions, these data show no obvious strong correlation between B-value and depth, nor b-value and Δmag.

Interactive 4-D (space/time) visualization of Alaska seismicity: Assessing the spatial and temporal behavior of seismicity in Alaska is more challenging than in, for example, California, because of Alaska's large spatial expanse, the temperature extremes that can inhibit easy access to seismic stations that require maintenance and the non-uniform station spacing and recording capabilities. To help improve our intuitive understanding of the last 20 years of Alaska seismicity we created a *scene file* of the 14725 earthquakes in our data set (M≥4 hypocenters; 1901-2015), which can be interactively viewed using the QPS *FLEDERMAUS* software suite that runs on any platform (e.g., Windows, Mac, Linux) using the iVeiw4D freeware. In this way, a user can explore the spatial and temporal evolution of these data interactively [Kilb et al., 2003]. Using this freeware and *scene file* anyone can view these data while freely zooming, panning and rotating through a 3-D view of the data's spatial extent (Figure 7). Using this data exploration tool we find the following: (1) Color-coding the events by time of day we find no strong time-of-day dependence within the data that might be indicative of anthropogenic activity; (2) Many events have a depth of 33km, indicating these depths are not well constrained [USGS FAQ, 2016]. (3) By color-coding the events by time we can seismic

activity is continual throughout the subduction zone. (4) The dip of the subduction zone is not uniform throughout the region, but varies a long strike. In summary, although we could have discerned these features using histograms and data-subsets, the interactivity of viewing the data both spatially and temporally simultaneously allowed us to more quickly and efficiently gain an understand of the Alaska seismicity.

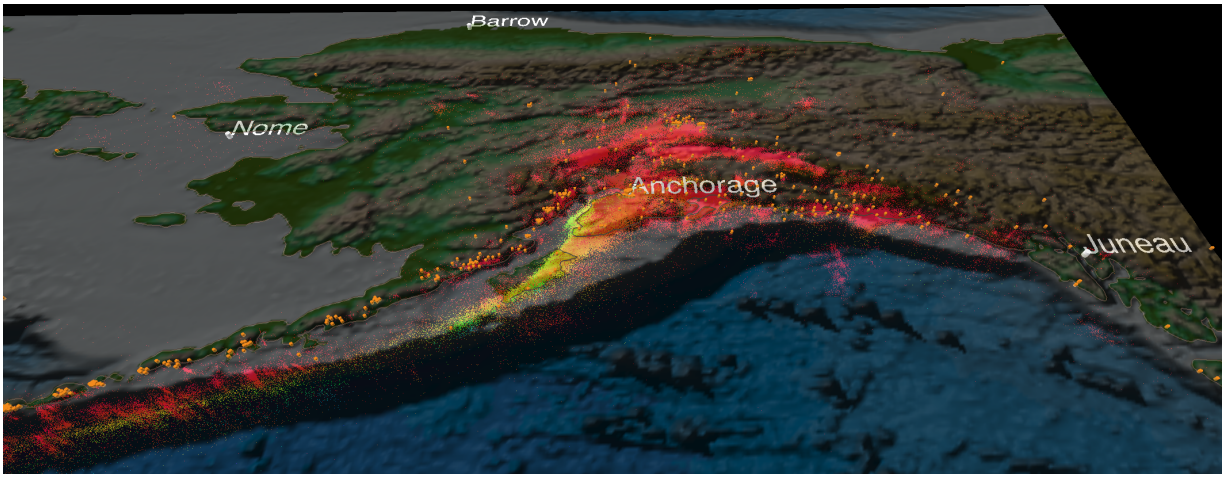

Figure 7: Snapshot from an interactive visualization of earthquake data from the Alaska region. Earthquakes are depicted as colored points, here color-coded by depth. Yellow points indicate deeper depths, highlighting the Alaskan subduction zone.

Conclusions

The seismic hazard risks in Alaska, from both mainshocks and large aftershocks, are among some of the highest in the nation and pose tsunamigenic risks as well [Lay et al., 2011]. In this work we use masinshock/aftershock sequence data from 50 large events (M≥6.5) in Alaska within the last 20 years to help inform hazard mitigation strategies. To improve our understanding of our data's spatial and temporal behavior we created an interactive visualization of our data (14725 M≥4 hypocenter locations; 1901-2015) using a 4-D (space and time) *scene file* that allows one to zoom, pan and rotate to explore these data in more detail. This type of interactive exploration was particularly useful for these data because of the vast mapped distribution of the data (70° by 30°) and large span of earthquake depths (0-300 km).

Of the 50 mainshocks in our study (M≥6.5; 1995-2015), 7 we deem either pre-shocks or aftershocks of other earthquakes and do not consider these 7 mainshocks in our analysis. Of the remaining 43 mainshocks, the large variation in depths, non-uniformity of station spacing and coverage and variation in catalog completeness makes it difficult to find a one-size-fits all clustering method to identify aftershocks. We therefore take an alternative approach and identify sequences that have a ΔMag value that remains the same throughout reasonable variations in the spatial footprint (within ±2°) and temporal duration (within 30 days) of the aftershock sequence. In this way we

identified 27 mainshocks that have robust Δmag values, these preferred events were the focus of our study.

Our primary findings include: (1) We net a range of Δmag values (0.1-2.7) that have a median value of 1.1, which is consistent with Bath's law. (2) For shallow mainshocks (depths ≤50 km) there is no correlation between depth and Δmag, but the two deepest events (mainshock depths that exceed 100 km; 109 km, M7.9 2014; and 134 km, M6.6, 2001) have relatively larger Δmag values (1.9 and 2.5, respectively). (3) The spatial distribution of Δmag weakly suggests a tendency for lower differentials for events in the Aleutians, higher differentials in south-central Alaska and average differentials in southeast Alaska. (4) We find no obvious correlation between B-value and depth, nor B-value and Δmag. However, there are too few sequences, only 7, that have a robust B-value (standard deviations < 0.2; 50 or more aftershocks in the sequence) to make any strong conclusion.

Based on this work we conclude that aftershock seismic hazard risk for the Alaska region should not rely on a 'one size fits all' method, and to start, aftershock hazards for deep mainshocks (>100 km) be treated differently than shallow mainshocks. Data collected by EarthScope's USArray in Alaska will likely record additional data that will aid in determining how to assess aftershock seismic hazard risks in Alaska, especially those within subduction zone settings.

Appendix A

Table A: Listing of 50 mainshock events (1995-2015) used in this study. Events are ordered by date, where older events are listed first. Events deemed either a pre-shock or after-shock of another event are flagged for removal (shaded in gray) and for these events we not compute Δmag, b-value or b-value standard deviation values (indicated by the '—' symbol). The Δmag and b-values values that are the most robust are shaded green (27) and orange (7), respectively. Non-robust values are also listed (not color-coded). An identification index number (left column) is assigned to each event and used in Figures 4 and 6.

Index	Date/Time	Mag	Lat	Lon	Depth (km)	# AS	Δmag	b-value	b-val std
1	23-Apr-1995 02:55:56	6.5	51.35	-180.3	15.1	18	1.8	0.84	0.21
2	22-Mar-1996 03:24:21	6.7	51.32	-181.3	20	29	--	--	--
3	22-Mar-1996 04:46:11	6.7	51.17	-181.1	44.4	20	--	--	--
4	08-Jun-1996 23:19:17	6.5	51.45	-178.1	43.3	193	--	--	--
5	10-Jun-1996 04:03:36	7.9	51.59	-177.6	28.7	197	0.6	0.73	0.05
6	10-Jun-1996 15:24:58	7.3	51.43	-176.8	27.3	127	0.7	0.82	0.07
7	10-Jun-1996 15:36:33	6.6	51.17	-176.7	52.5	126	--	--	--
8	26-Mar-1997 02:08:58	6.7	51.27	-180.5	29.3	27	1.1	0.73	0.14
9	17-Dec-1997 04:38:53	6.6	51.20	-181.1	21	19	1.0	0.63	0.14
10	28-Jan-1999 08:10:06	6.6	52.89	-169.1	68.6	6	2	0.67	0.40
11	20-Mar-1999 10:47:48	6.9	51.59	-177.7	45.6	8	2.2	0.61	0.28
12	06-Dec-1999 23:12:34	7.0	57.35	-154.5	58.5	14	0.6	0.48	0.12
13	11-Jul-2000 01:32:28	6.5	57.41	-154.4	49	2	1.0	0.79	0.72
14	10-Jan-2001 16:02:43	6.9	56.93	-153.5	25	6	1.6	0.38	0.13
15	14-Jun-2001 19:48:49	6.5	51.16	-179.9	18	6	1.5	0.49	0.20
16	28-Jul-2001 07:32:44	6.6	59.00	-155.1	135	2	2.5	0.33	0.32
17	23-Oct-2002 11:27:20	6.6	63.53	-148.2	13	74	--	--	--
18	03-Nov-2002 22:12:43	7.8	63.54	-147.7	19	77	2.7	1.14	0.17
19	07-Nov-2002 15:14:07	6.6	51.15	-180.7	26	21	1.6	0.86	0.21
20	19-Feb-2003 03:32:37	6.6	53.60	-164.7	19	8	1.7	0.71	0.35
21	17-Mar-2003 16:36:18	7.0	51.28	-182.1	28	23	0.9	0.56	0.11
22	15-Jun-2003 19:24:34	6.5	51.56	-183.2	20	18	--	--	--
23	23-Jun-2003 12:12:35	6.9	51.46	-183.3	20	15	1.9	0.69	0.20

24	17-Nov-2003 06:43:07	7.8	51.12	-181.4	29.9	188	2	0.83	0.05
25	28-Jun-2004 09:49:47	6.8	54.80	-134.5	16	2	1.8	0.46	0.43
26	14-Jun-2005 17:10:12	6.8	51.21	-180.6	17	27	1.2	0.75	0.15
27	14-Jun-2006 04:18:42	6.5	51.72	-182.9	14	32	0.3	0.66	0.12
28	08-Jul-2006 20:40:00	6.6	51.23	-179.3	22	30	1.2	0.52	0.06
29	02-Aug-2007 03:21:42	6.7	51.26	-179.9	21	20	1.1	0.69	0.17
30	15-Aug-2007 20:22:10	6.5	50.28	-177.5	9	19	0.7	0.78	0.20
31	19-Dec-2007 09:30:27	7.2	51.36	-179.5	34	48	0.9	0.49	0.05
32	05-Jan-2008 11:01:06	6.6	51.254	-130.8	15	13	0.2	0.47	0.14
33	16-Apr-2008 05:54:19	6.6	51.878	-179.2	13	19	0.0	0.67	0.19
34	02-May-2008 01:33:37	6.6	51.864	-177.5	14	10	1.7	0.65	0.23
35	13-Oct-2009 05:37:23	6.5	52.754	-167.0	24	16	0.1	0.41	0.07
36	17-Nov-2009 15:30:47	6.6	52.123	-131.4	17	6	0.8	0.64	0.33
37	30-Apr-2010 23:11:43	6.5	60.473	-177.9	12	6	0.2	0.40	0.17
38	18-Jul-2010 05:56:44	6.7	52.876	-169.9	14	104	0.7	1.06	0.11
39	03-Sep-2010 11:16:06	6.5	51.451	-175.9	23.5	3	2.1	0.43	0.33
40	24-Jun-2011 03:09:39	7.3	52.05	-171.8	52	31	1.5	0.65	0.12
41	02-Sep-2011 10:55:53	6.9	52.171	-171.7	32	23	1.3	0.61	0.12
42	28-Oct-2012 03:04:08	7.8	52.788	-132.1	14	185	1.5	1.05	0.09
43	05-Jan-2013 08:58:19	7.5	55.394	-134.7	10	19	1.6	0.59	0.16
44	30-Aug-2013 16:25:02	7.0	51.537	-175.2	29	115	0.5	0.64	0.05
45	04-Sep-2013 02:32:30	6.5	51.557	-174.8	20	62	--	--	--
46	24-Apr-2014 03:10:10	6.5	49.639	-127.7	10	7	1.7	0.59	0.26
47	23-Jun-2014 20:53:09	7.9	51.849	-181.3	109	109	1.9	0.88	0.10
48	29-May-2015 07:00:09	6.7	56.594	-156.4	72.6	5	1.5	0.46	0.23
49	27-Jul-2015 04:49:46	6.9	52.376	-169.5	29	71	1.0	0.70	0.08
50	09-Nov-2015 16:03:46	6.5	51.639	-173.1	15	8	1.3	0.61	0.26

References

Aki, K. [1965], Maximum likelihood estimate of b in the formula log N = a − bM and its confidence limits, *Bull. Earthquake Res. Inst.* Tokyo Univ., 43, 237–239.

Bath, M. [1965]. Lateral inhomogeneities of upper mantle, *Tectonophysics,* 2, 483–514, doi:10.1016/0040-1951(65)90003-X.

Bender, B. [1983]. Maximum likelihood estimation of b-values for magnitude grouped data. *Bull. Seismol. Soc. Am.* 73, 831–-851.

Console, R., A. M. Lombardi, M. Murru, and D. Rhoades [2003]. Båth's law and the self-similarity of earthquakes, *J. Geophys. Res.,* 108, 2128, doi:10.1029/2001JB001651.

DeMets, C., Gordon, R. G., Argus, D. F., & Stein, S. [1994]. Effect of recent revisions to the geomagnetic reversal time scale on estimates of current plate motions. *Geophysical research letters*, *21*, 2191-2194.

Elliott, J.. J.T. Freymueller, and C.F. Larsen [2013]. Active tectonics of the St. Elias orogen, Alaska, observed with GPS measurements, *J. Geophys. Res.,* V 118, Pages 5625–5642, DOI: 10.1002/jgrb.50341

Felzer, K. R., [2006]. Calculating the Gutenberg-Richter b value, *American Geophysical Union, Fall Meeting 2006*, abstract #S42C-08.

Felzer, K. R., R. E. Abercrombie, and G. Ekström, [2003]. Secondary aftershocks and their importance for aftershock prediction, *Bull. Seis. Soc. Am.*, 93, 1433-1448.

Freymueller, J. T. (2012), Observation of a "Locking Event": A newly observed transient variation in the pattern of slip deficit at the Alaska Subduction Zone, *Seismol. Res. Lett.,* 83, 433.

Freymueller, J.T., Cohen, S.C., Cross, R., Elliott, J., Fletcher, H.J., Larsen, Hreinsdottir, S. & Zweck, C. [2008]. Active deformation processes in Alaska, based on 15 years of GPS measurements, in AGU Geophys. Mono.. eds Freymueller, J.T., Haeussler, P.J., Wesson, R.W. & Ekstrom, G., American Geophysical Union, 179, 350 pp.

Gerstenberger M., S. Wiemer, L. M Jones, P. A Reasenberg [2005]. Real-time forecasts of tomorrow's earthquakes in California*, Nature* **435**, 328-331 doi:10.1038/nature03622.

Ghosh, A., A. V. Newman, A. M. Thomas, and G. T. Farmer [2008]. Interface locking along the subduction megathrust from b-value mapping near Nicoya Peninsula, Costa Rica, *Geophys. Res. Lett.,* 35, L01301,doi:10.1029/2007GL031617.

Glasscoe, M.T., J .Wang, M. E. Pierce, et al. [2014]. E-DECIDER: Using Earth Science Data and Modeling Tools to Develop Decision Support for Earthquake Disaster Response, *Purr Apple. Geophys.* DOI 10.1007/s00024-014-0824-9.

Gomberg, J. and B. Sherrod [2014]. Crustal earthquake triggering by modern great earthquakes on subduction zone thrusts. *J. Geophys. Res.,* 10.1002/2012JB009826.

Gomberg, J., and S. Prejean [2013]. Triggered tremor sweet spots in Alaska. *J. Geophys. Res.,* 118(12), 6203-6218.

Gutenberg, B., and C. Richter [1944]. Frequency of earthquakes in California, Bull. *Seismol. Soc. Am.,* 34, 185–188.

Hanizl, S. [2013]. Comment on **"**Self-similar earthquake triggering, Båth**'**s law, and foreshock/aftershock magnitudes: Simulations, theory, and results for southern California**"** by P. M. Shearer, *J. Geophys. Res.,* 118, doi:10.1002/jgrb.50132.

Helmstetter, A., and D. Sornette [2003]. Båth's law derived from the Gutenberg-Richter law and from aftershock properties, *Geophys. Res. Lett.*, **30**(20), 2069, doi:10.1029/2003GL018186.

Kilb, D., C.S. Keen, R.L. Newman, G.M. Kent D.T. Sandwell, F.L. Vernon, C.L. Johnson, and J.A. Orcutt [2003]. The visualization center at Scripps Institution of Oceanography: Education and Outreach, *Seismol. Res. Lett.,* 74, 641-648, 10.1785/gssrl.74.5.641.

Lay, T., C. J. Ammon, H. Kanamori, Y. Yamazaki, K. F. Cheung, and A. R. Hutko [2011], The 25 October 2010 Mentawai tsunami earthquake (Mw 7.8) and the tsunami hazard presented by shallow megathrust ruptures, *Geophys. Res. Lett.*, 38, L06302, doi:10.1029/2010GL046552.

Lombardi, A.M., [2002]. Probabilistic interpretation of Baths' Law. *Annals of Geophyscis,* V45.

Peterson, C. L., and D. H. Christensen [2009], Possible relationship between nonvolcanic tremor and the 1998–2001 slow slip event, south central Alaska, *J. Geophys. Res.,* 114, B06302.

Reasenberg, P.A., and L.M. Jones [1989]. Earthquake Hazard After a Mainshock in California, *Science*, 243, 1173-1176.

Ruppert, N. A., Lees, J. M., & Kozyreva, N. P. [2007]. Seismicity, Earthquakes and Structure Along the Alaska-Aleutian and Kamchatka-Kurile Subduction Zones: A Review. *Volcanism and Subduction: The Kamchatka Region*, 129-144.

Schorlemmer, D., S. Wiemer, and M. Wyss [2005]. Variations in earthquake**-**size distribution across different stress regimes, *Nature,* 437(7058), 539**–**542, doi:10.1038/nature04094.

Shcherbakov, R., K Goda, A Ivanian, GM Atkinson [2013]. Aftershock Statistics of Major Subduction Earthquakes, *Bull. Seismol. Soc. Am.,* 103, 3222-3234.

Shearer, P. M. [2012]. Self-similar earthquake triggering, Båth**'**s law, and foreshock/aftershock magnitudes: Simulations, theory, and results for southern California, *J. Geophys. Res.,* 117, B06310, doi:10.1029/2011JB008957.

Skyes, L. R. [1971]. Aftershock Zones of Great Earthquakes, Seismicity Gaps, and Earthquake Prediction for Alaska and the Aleutians, *J. Geophys. Res.,* 76, 8021-8041.

Tormann, T., S. Wiemer, and A. Mignan [2014]. Systematic survey of high-resolution b value imaging along Californian faults: Inference on asperities. *J. Geophys. Res, 119, 2029–2054, doi:10.1002/2013JB010867.*

USGS FAQ, [2016]. https://www2.usgs.gov/faq/categories/9826/3427

Wessels, S. A., De La Pena, A., Kratz, M., Williams-Stroud, S., & Jbeili, T. [2011]. Identifying faults and fractures in unconventional reservoirs through microseismic monitoring. *First break*, *29*(7), 99-104.

Wiemer, S., and M. Wyss [2002]. Mapping spatial variability of the frequency-magnitude distribution of earthquakes, *Adv. Geophys.,* 45, 259–302.

4. Bibliography: List of publications resulting from the work performed under the award.

Kilb, D, ASSESSING THE HAZARD OF LARGE AFTERSHOCKS IN ALASKA, Seismological Society of America (SSA), Poster #60, 2016.

Kilb, D., Assessing the hazard of large aftershocks in Alaska, manuscript in preparation for submission to SSA, 2016.